

ARTICLE



Synaptic noise facilitates the emergence of self-organized criticality in the *Caenorhabditis elegans* neuronal network

K. Çiftçi

Biomedical Engineering Department, Çorlu Faculty of Engineering, Tekirdağ Namık Kemal University, Çorlu, Tekirdağ, Turkey

ABSTRACT

Avalanches with power-law distributed size parameters have been observed in neuronal networks. This observation might be a manifestation of self-organized criticality (SOC). Yet, the physiological mechanisms of this behaviour are currently unknown. Describing synaptic noise as transmission failures mainly originating from the probabilistic nature of neurotransmitter release, this study investigates the potential of this noise as a mechanism for driving the functional architecture of the neuronal networks towards SOC. To this end, a simple finite state neuron model, with activity dependent and synapse specific failure probabilities, was built based on the known anatomical connectivity data of the nematode *Caenorhabditis elegans*. Beginning from random values, it was observed that synaptic noise levels picked out a set of synapses and consequently an active subnetwork that generates power-law distributed neuronal avalanches. The findings of this study bring up the possibility that synaptic failures might be a component of physiological processes underlying SOC in neuronal networks.

ARTICLE HISTORY

Received 7 February 2018
Accepted 10 October 2018

KEYWORDS

Self organization; criticality;
Caenorhabditis elegans;
neuron; network; synapse;
noise

Introduction

Synaptic transmission in neurons exhibits a fair amount of randomness. This random behaviour mainly originates from the probabilistic nature of quantal release, the random nature of diffusion and chemical reactions within the synaptic cleft, and the unpredictable responses of ligand-gated ion channels (White and Rubinstein 2000). In most cases, a synapse is more likely to fail to release transmitter in response to an incoming signal (Laughlin and Sejnowski 2003). The influence of noise on communication systems is rather complex and may lead to some unexpected improvements in system capabilities (Jung and Hnggi 1991). In the same manner, the synaptic noise was shown to advance learning capabilities of the neural network (Buhmann and Schulten 1987), maximize information storage capacity (Varshney et al. 2006), and improve information transmission between neural populations (Gatys et al. 2015). Based on this regulatory effects of synaptic noise in neural

systems, the research described here set out to explore the influence of noise on the self organized critical behaviour of neural systems.

SOC has been hypothesized to be a fundamental property of neural systems (Hesse and Gross 2014). Activity in the brain displays many different scales of organization, yet without a central executive. SOC theory (Bak and Wiesenfeld 1987) underlines the propensity of some systems, generally consisting of large number of interacting entities, to drive themselves to criticality where they function at the edge of phase transitions. This critical regime equips the systems with the potential to develop extended correlations in time and space, which, in the sequel, drives the emergence of global behaviour from local interactions. The existence and emergence of SOC in the brain has been investigated both experimentally (e.g., Beggs and Plenz 2003; Linkenkaer-Hansen et al. 2001) and theoretically (e.g., Wang et al. 2011; Lin and Chen 2005). Activity-dependent synaptic plasticity has been investigated as a possible mechanism of self tuning towards SOC (Levina 2008; Meisel and Gross 2009; Droste et al. 2012). Neuron level synaptic plasticity generates a network level dynamic topology (and vice versa) that provides the local neurons with global information which is critical for SOC behaviour.

Avalanches whose size parameters are distributed according to power-law is the main manifestation of the SOC. Models based on SOC was shown to be able to reproduce the power-law behaviour of experimental data (de Arcangelis et al. 2006). Power law is interesting because, from a qualitative perspective, although the majority of the avalanches are small in size, there is a finite possibility of observing middle and big sized, even reaching to the system size, avalanches. This tailors a complex interaction among network members. In subcritical systems the interactions are mainly local whereas in supracritical systems local activations quickly spread out to the whole system. On the other hand, in the critical systems there are both activations confined to a small region and global cascades. This type of behaviour suits very well with the observed segregation/integration balance (Tononi et al. 1994) and small-world regime (Achard et al. 2006) of the neuronal networks. It has been conjectured that topological properties of local cortical circuits governed by some simple wiring rules might be important for the emergence of power-law statistics (Teramae and Fukai 2007).

Caenorhabditis elegans is known to have a small-world neuronal network (Amaral et al. 2000), and small world networks exhibit a SOC behaviour (Lin and Chen 2005). The present study aims at exploring the potential of synaptic noise to drive neural systems, and particularly *C. elegans* neuronal network, towards SOC. The starting hypothesis was that the plasticity induced by an adaptive synaptic noise process might bring out a functional network topology, which exhibited neuronal avalanches. Using a simple discrete model based on the neuronal anatomical connectivity of *C. elegans*,

the synaptic failures were shown to be indeed essential for sustaining the network activity at a critical regime.

Methods

The anatomical network

A near complete description of the nematode *C. elegans* nervous system has been achieved using electron microscopy reconstructions (Varshney et al. 2011), and is freely available online.¹ *C. elegans* possesses 302 neurons of which 282 are somatic and 20 are pharyngeal. Three of the somatic neurons do not make any synapses. The remaining 279 somatic neurons make 514 gap junction connections and 2194 chemical synapses. In the current study, the full network formed by bringing together both types of synapses, was analysed. Since the directionality of gap junctions was not available these contacts were treated as bidirectional whereas the directionality of chemical synapses were conserved. In total, this procedure generated a network of 279 neurons with 2990 directed edges. Please note that this is the network denoted as the full network in Varshney et al. (2011).

The model

The spreading of forest fires was one of the first applications of SOC analysis (Drossel and Schwabl 1992). The forest fire model has been particularly useful because it easily lends itself to describe dynamically similar albeit different systems. Accordingly, similar models were used to describe activation spreading in a network of neurons (Muller-Linow et al. 2008; Droste et al. 2012). The model is simplistic in the sense that a neuron, at any time, can be in any one of the three states: susceptible (S), excited (E), and refractory (R). In this study, synaptic failures were included in the model with their corresponding probability. The evolution of the model is described by the following rules:

- A susceptible neuron can go into the excited state spontaneously with probability f .
- A neuron can also be activated by one of its incoming neighbours.
- A synapse may fail to transmit the activity with an adaptive probability g .
- After the excited state, a neuron enters into the refractory state.
- The neuron can recover from the refractory state and become a susceptible neuron with probability q .

SOC is generally inspected through observing avalanche dynamics. After a slow and long driving process, a fast avalanche event (in our case successive

excitation of neurons) with short duration occurs. Several orders of magnitude difference between time scales of the accumulation and avalanche periods is a characteristic feature of SOC. This difference is reflected in the separation of scales and is usually achieved by setting $q \gg f$. Introducing the parameter,

$$\theta = q/f, \quad (1)$$

this ratio was set to 10, 20, 50, 100, 200, 300, 500 and 1000 in this study. In the implementation, this corresponds to making θ random attempts to carry refractory neurons to susceptible state, i.e. the driving phase, which is followed by a random selection of a neuron for excitation. If the selected node is a susceptible node, then an avalanche starts, the constant driving stops and the avalanche travels according to neighbourhood relations. This continues until all network activations come to an end. Accordingly, θ determines the expected time length between avalanches. The extent of the avalanche was determined by a breadth-first search algorithm (Grassberger 2002).

The synaptic noise, reflected by the synaptic failure probability, g , is the main driving force of the functional network topology. This probability was allowed to vary depending on the avalanche formation. During an avalanche an activated node may not be able to trigger an activation in any of its outgoing susceptible neighbours because of two reasons: That node may have been already activated by another neighbouring node or synaptic failure may not allow the transmission of activity. Accordingly, when two neighbouring nodes are both activated but the synapse between them is not the carrier of this activity, the synaptic failure probability of this synapse is increased by

$$\Delta g = \mu_1 f_1(s)(1 - g), \quad (2)$$

where μ_1 is the constant step parameter, and f_1 is a function depending on the avalanche size (s) and defined as $f_1 = 1 - 1/s$. Consequently, when two neighbouring susceptible nodes are both activated via their shared synapse, the synaptic failure probability is updated as follows:

$$\Delta g = -\mu_2 f_2(s)g, \quad (3)$$

where μ_2 is again the constant step parameter, and f_2 is an avalanche size-dependent function defined as $f_2 = 1/s$. The determination of f_1 and f_2 is mainly heuristic: Consider that an avalanche is formed by activated neurons and the synapses among them. Some synapses are the members of the avalanche because they propagate the activation, whereas some others are not, because they are not able to transmit the activity because of the aforementioned reasons. We conjectured that the failure probability increments of an omitted synapse should grow with increasing avalanche size, whereas failure probability decrements should get smaller with increasing avalanche sizes. In other words, small avalanches should be more selective for successful synapses while large avalanches should be more selective for failing synapses. However, with these choices of f_1

and f_2 , the failure probability increments would always be higher than those of decrements for avalanches occupying more than 2 neurons. The constants μ_1 and μ_2 cope with this imbalance. μ_2 values bigger than μ_1 keep the update steps of decrements larger than increments for a longer period. In this study μ_1 and μ_2 were set to 0.1 and 0.8, respectively. Rather than the absolute values, the ratio is important for the performance. With these parameter settings, the change in the update parameters with increasing avalanche size is shown in Figure 1. Accordingly, our update rule depends on the avalanche size and hence is non-local. It should also be noted that our selection of the update functions enable a soft bound on the synaptic failure probability between 0 and 1 and the update steps depend on the current value. Figure 2 shows the avalanche formation and synaptic failure updates on a simple network.

Simulations and data analysis

Simulations and all related analyses were performed using Python with Numpy, Scipy (Jones et al. 2001) and Matplotlib (Hunter 2007) packages. Graph-theoretical analysis was used to relate the simulation results to the network structure. For this purpose custom-written codes with Python using Networkx package (Hagberg et al. 2008) were used. Each neuron was defined as a node of the graph and each synapse was assigned to an edge. The terms neuron/node and edge/synapse are used interchangeably throughout this paper.

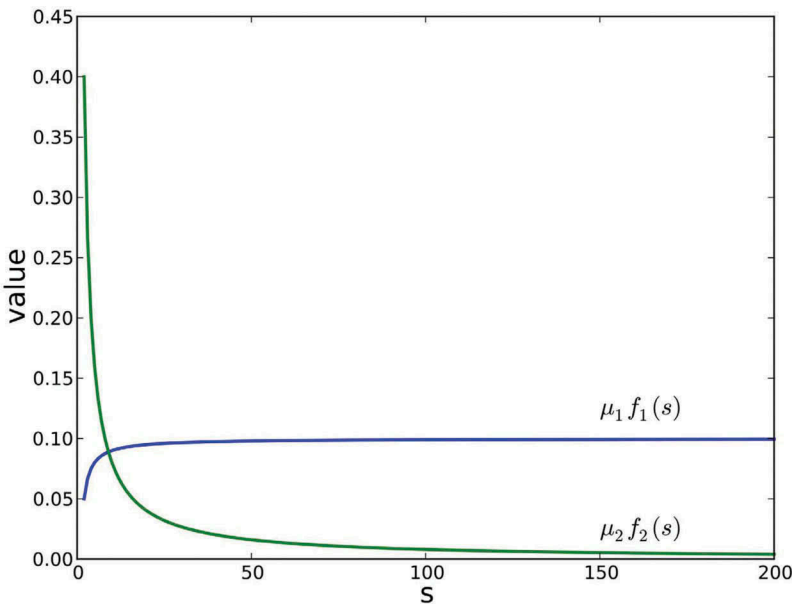


Figure 1. The change in total update parameter, $\mu_k f_k$ with avalanche size (s).

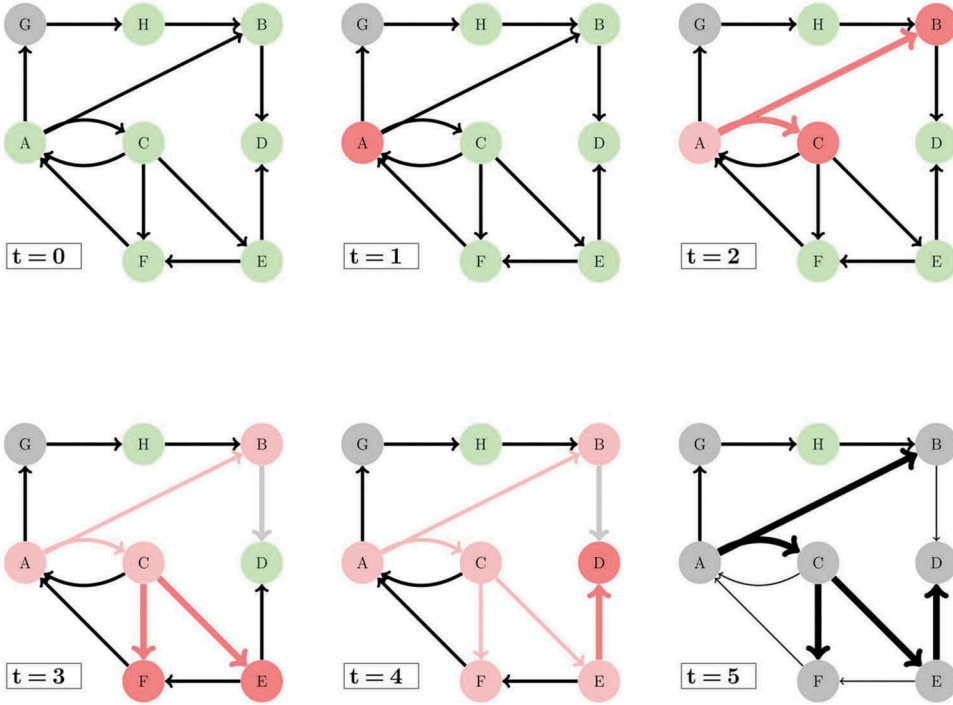


Figure 2. At $t = 0$, all the nodes but node G are in susceptible state, and let's assume that failure probabilities for all synapses are the same. At $t = 1$, node A becomes activated. At $t = 2$, nodes C and B are activated via node A. But node G cannot be activated since it is in the refractory state. At $t = 3$, nodes E and F are activated via node C, but synapse between B and D fails. At $t = 4$ node D is activated via node E. At $t = 5$ all the nodes but node H are in the refractory state. The failure probabilities of synapses A–C, A–B, C–F, C–E and E–D get lower (synaptic connections get stronger). The failure probabilities of C–A, F–A, E–F and B–D get higher, since they connect activated nodes but they are not the carriers of these activations. Synaptic strengths of A–G, G–H and H–B do not change, because they do not connect pairs of activated nodes.

The assessment of SOC was done mainly via fitting a power-law distribution, ($p(s) \propto s^{-\alpha}$), to the two parameters estimated from the avalanche: First, the avalanche size measured as the total number of neurons activated during an avalanche and second the eccentricity, i.e. the longest path length between any two nodes of the subnetwork. Additionally, it was checked whether the avalanche size was comparable to the network size. For fitting power-law distribution, the procedure described in the seminal paper of Clauset et al. (2009) was adopted. In summary, the scaling parameter, α was estimated with the method of maximum likelihood. A Kolmogorov–Smirnov (KS) statistic was computed for this fit. After generating synthetic data sets using the same scaling parameter, KS statistic was determined for each dataset. The null hypothesis was that our original data came from a power-law distributed variable. To be able to reject the null hypothesis, the original KS statistic of the empirical data should be significantly higher than those of the synthetic

data. This is simply evaluated by determining what fraction of the time the synthetic statistic is larger than the value for the empirical data. Denoting this fraction as the p -value, the null hypothesis was rejected if $p \leq 0.1$.

Results

Case 1: No synaptic noise

Before beginning our exposition about the effect of noise on the SOC behaviour of *C. elegans* network, it would be informative to inspect the no-noise case. For this purpose the failure probability was set to 0 for all synapses and the simulation runs were repeated for 20 times. Figure 3 shows the avalanche sizes for different θ values. It may be clearly observed that especially beginning with $\theta = 50$ characteristic scale(s) for avalanches occur. Although, the relation of these avalanche scales to network topology is a matter of interest, since the primary concern of this paper is the emergence of SOC behaviour, we will leave this topic for further studies and suffice by noting that when there is no synaptic noise the network operates in the supercritical regime.

The parameter θ determines the number of nodes that will be in the susceptible state after the driving period between the avalanches. If we denote

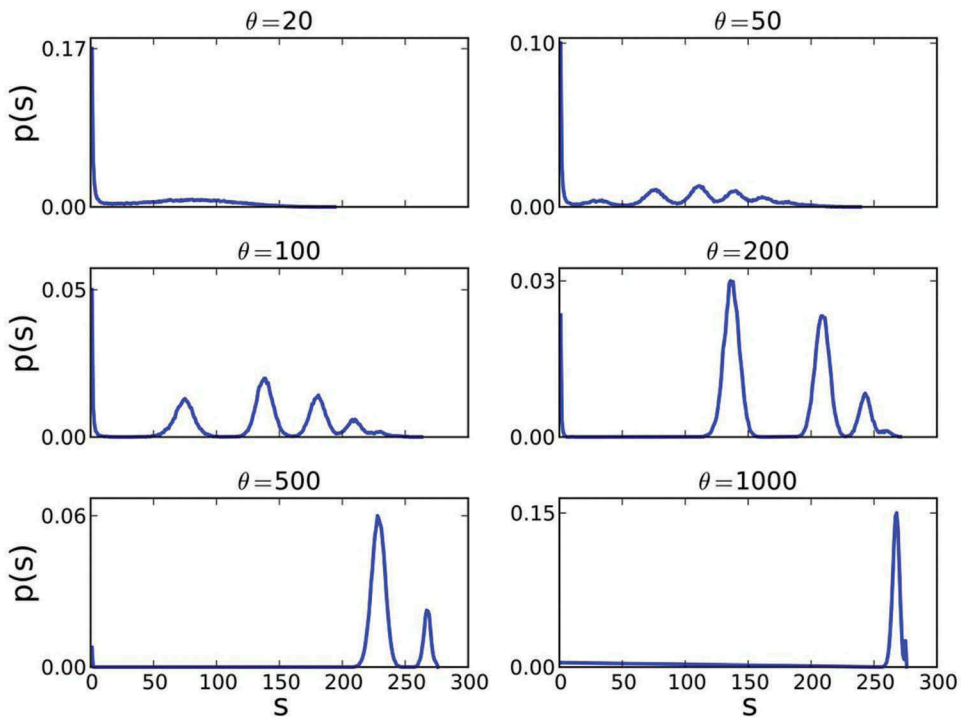


Figure 3. The avalanche sizes for no synaptic noise.

total number of nodes by N , a refractory node will be in the excited state with probability,

$$p = 1 - \left(\frac{N-1}{N}\right)^\theta. \quad (4)$$

Since the node selection is independent and uniformly distributed, this probability will also give the fraction of the nodes in the refractory state (assuming all of the nodes are refractory in the beginning). **Figure 4** quantifies this role of θ and it makes clear why at $\theta = 1000$ avalanche sizes are almost equal to the network size: Because almost all neurons are in the susceptible state. In the actual simulations, the number of susceptible neurons deviates from the numbers shown in this figure, because of the remaining susceptible neurons from the previous avalanche. The values of **Figure 4** actually constitute lower bounds.

Case 2: Adaptive synaptic noise

Simulations began with all nodes in the refractory state and failure probabilities were initially assigned to random values from a Gaussian distribution with mean 0.5 and standard deviation 0.05 . After the initialization, failure probabilities were updated for 40.000 avalanches and the convergence

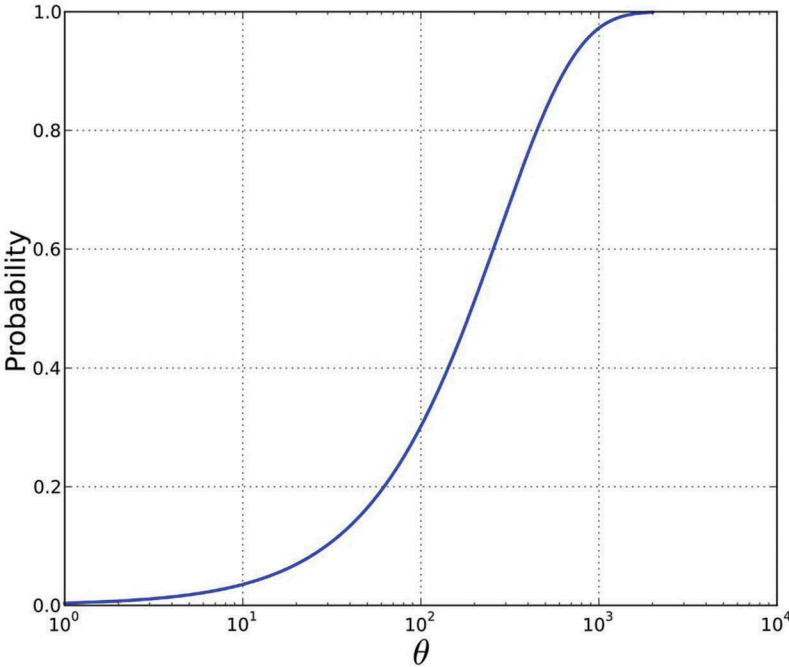


Figure 4. Assuming all nodes in the refractory state, the number of susceptible nodes after θ random refractory-susceptible transition attempts.

of these probabilities were observed. Afterwards, statistics of 10,000 avalanches were collected with fixed failure probabilities.

The convergence of the failure probabilities and the resulting values for a single run is presented in Figure 5. Defining G as the vector of individual synaptic failure probabilities, g , after every 100 avalanches, the relative sum squared change in the G were calculated. It may be observed that after about 30,000 avalanches convergence is attained. This convergence performance was valid for all θ values. The figure also exhibits the final failure probabilities for the corresponding run. Most of the resulting values converge to almost 1, whereas most of the remaining values converge to 0 with few values in between. In all the simulations, less than 400 (out of 2990) probability values converge to values less than 1. Although values close to 1 actually pruned away the corresponding edges, no node was excluded from the resulting network.

Figure 6 demonstrates the avalanche sizes measured as the total number of activated neurons, for different θ values. For small θ values, (< 100), the avalanche sizes begin to diverge earlier from the power law which is a manifestation of the subcritical dynamics. For θ values over 100, critical regime is attained (KS statistics with $p = 0.1$). The cut-off observed in the

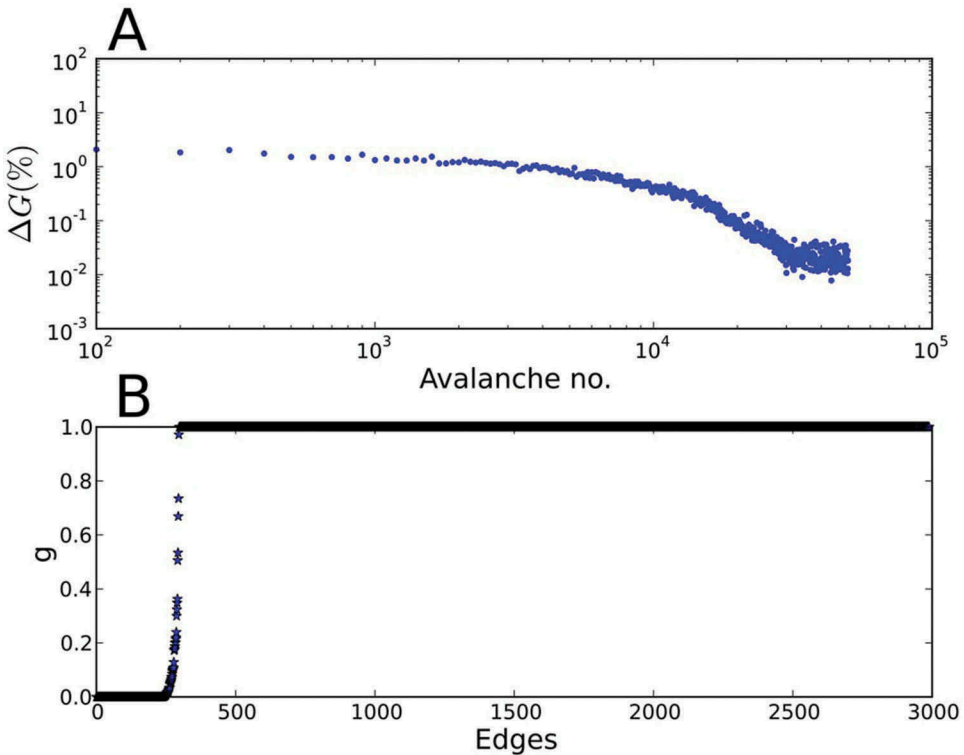


Figure 5. For a single run with $\theta = 300$, A. relative total change in the synaptic failure probability values, B. (sorted) final failure probability values.

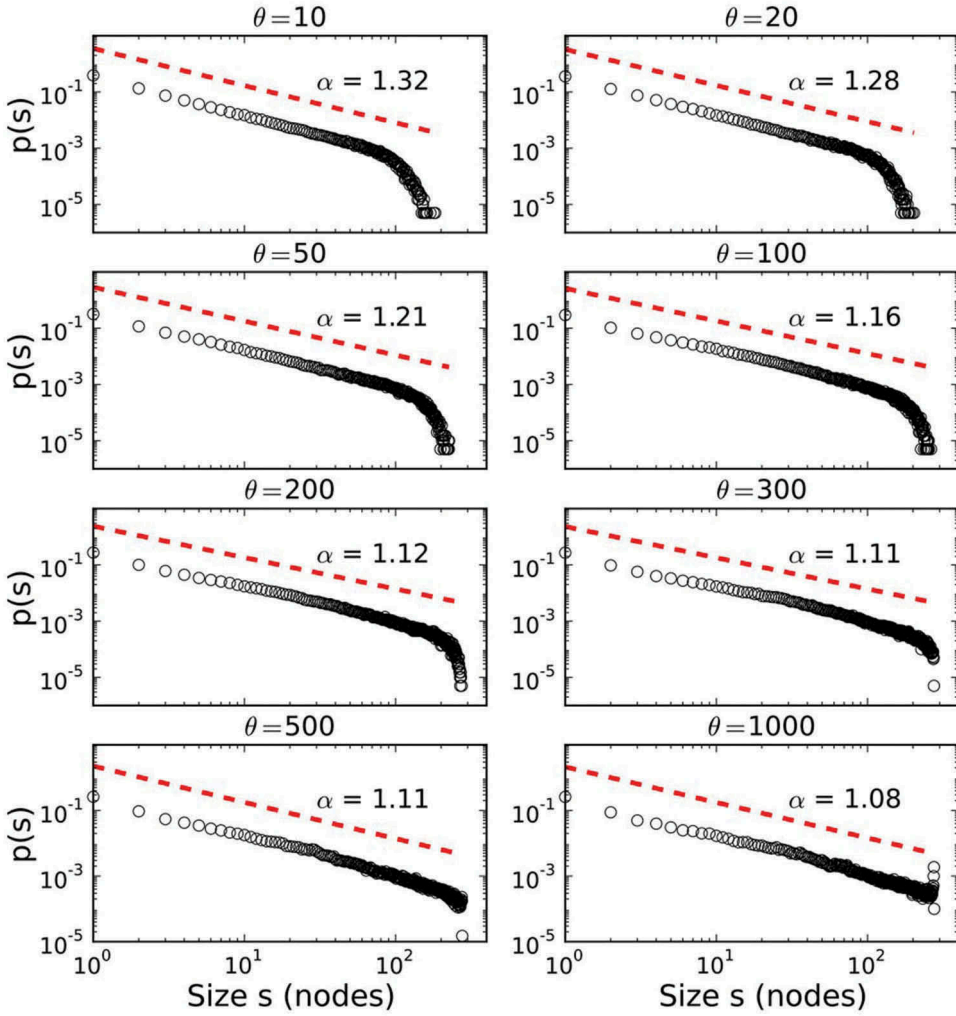


Figure 6. Empirical avalanche size (s versus probability ($p(s)$) and the power-law fit, ($p(s) = s^{-\alpha}$), graphs for different θ values.

avalanche size is due to the finite size of the network. For values close to 1000 the avalanche distribution begins to exhibit a sharp positive deflection close to the network size. We do not conceive this as an indication of the network entering into the supracritical regime, but rather again as a result of the limiting effect of the network size. To make this point clear, we carried the θ value to its utmost level, so as to make all neurons susceptible after each avalanche. The result was qualitatively similar and this observation corroborated our conjecture on the limiting effect of the network size. The difference between these three behaviours is more evidenced in [Figure 7](#).

The second size parameter investigated for the power-law was eccentricity. The activated nodes during an avalanche and the active synapses among

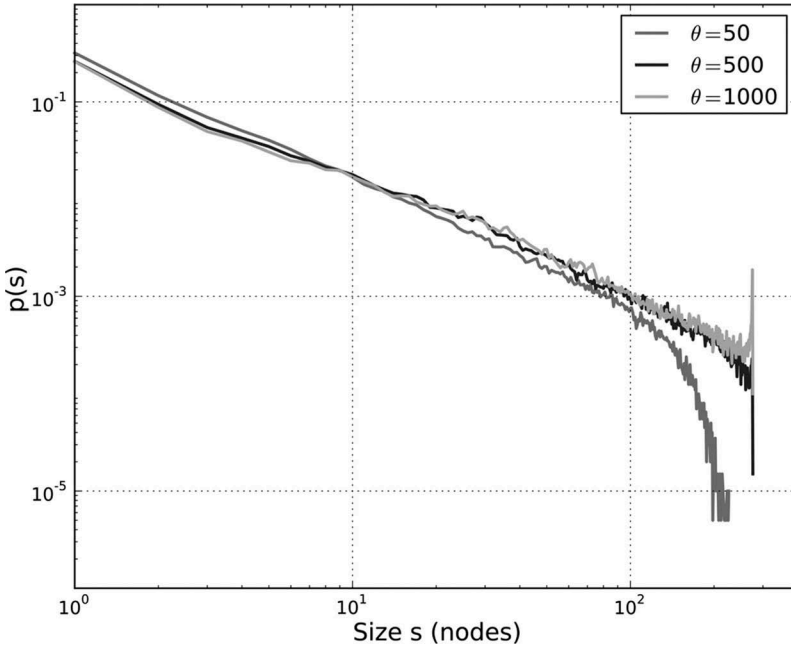


Figure 7. Redrawing of the avalanche size distributions for θ equal to 50, 500, and 1000.

them form a subgraph of the original graph. This subgraph was extracted at each avalanche event and the eccentricity, maximum path length between any two nodes, in this reduced network was determined. The results are presented in [Figure 8](#). The results are again indicative of a critical behaviour in the *C. elegans* network. Noting that the full network has an eccentricity value of 7, observed big eccentricity values point out to the long chains of neurons shaped by the synaptic noise levels.

The small size of *C. elegans* network poses some extra challenges to our ability to observe the critical dynamics. To corroborate the validity of our results, we resorted to a sensitivity analysis that was shown to be effective for small size social systems (Daniels et al. 2017). To this end, after their values converged, small perturbations were applied to the synaptic failure probabilities. Particularly, 1% of the synapses were randomly selected and their failure probabilities were altered 10% in absolute value. Then, the Kullback–Leibler divergence between the original neuronal activity distribution and the distribution of the perturbed network was calculated, and was normalized with the absolute change in the total failure probability. If the network is indeed driven into a critical regime with increasing θ values, then this should be also evident with the increasing sensitivity to perturbations. [Figure 9](#) shows that this is actually the case, with the sensitivity reaching a plateau at about $\theta = 200$.

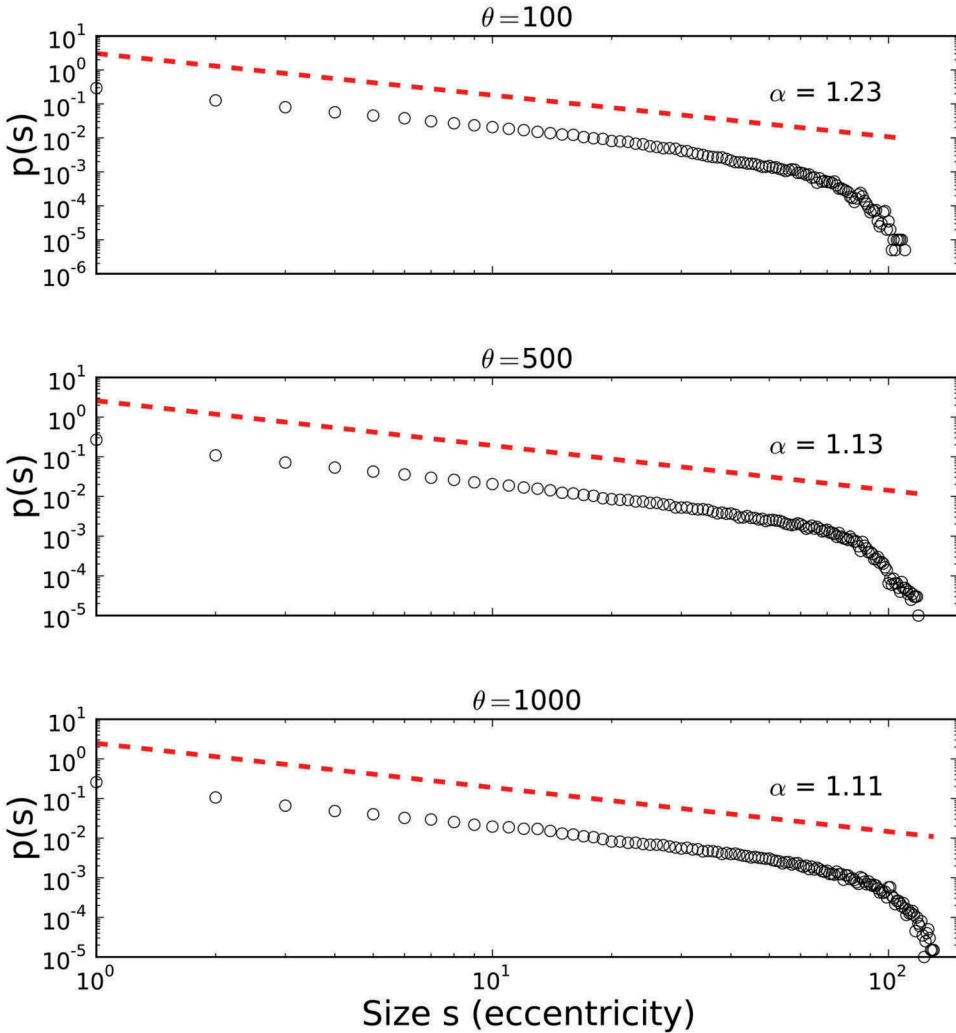


Figure 8. The eccentricity (maximum path length) for the avalanche subgraph for different θ values.

Relationships between neural dynamics and structure

A very important concern in neuroscience is the relationship between neural dynamics and the underlying structure. To be able to investigate these relations in our particular model, we made a series of analyses. To reiterate our simulation procedure, at each iteration a neuron is randomly selected and if it is in the susceptible state, it becomes activated and an avalanche begins. However, if the selected neuron is a refractory one, then no avalanche forms. Accordingly, we denoted avalanche initiation rate for a node as the ratio of actually starting an avalanche over total number of times being selected. Then, we inspected the correlation between the activation rate, i.e. average activation level for each neuron during a simulation run, and avalanche initiation rate. In

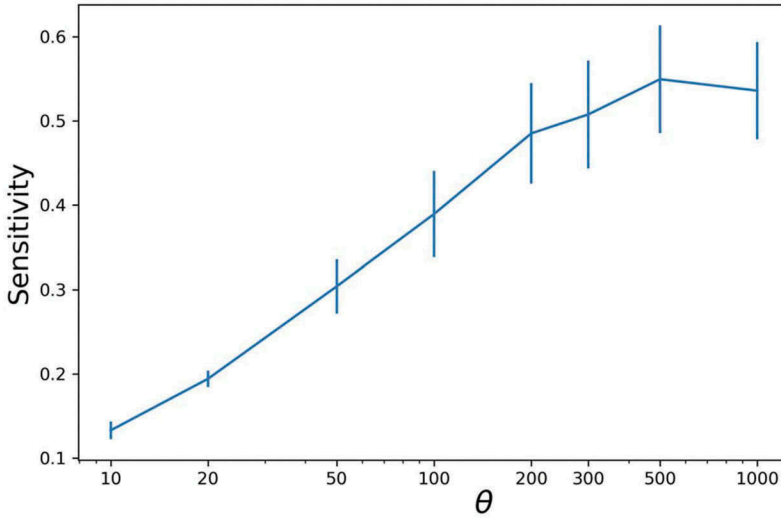


Figure 9. Change in the sensitivity of the network with increasing θ values. At each θ value, after convergence, the failure probabilities were perturbed 10 times, and this process was repeated 30 times for each θ . Figure shows the mean and the standard deviation of the normalized network sensitivity.

the simulations θ was fixed at 100. **Figure 10** shows that there is a significant negative correlation between these two rates ($r = -0.92, p < 0.001$). This is because highly activated nodes are more probable to be in the refractory state from the previous avalanches, and thus when selected, may not be able to

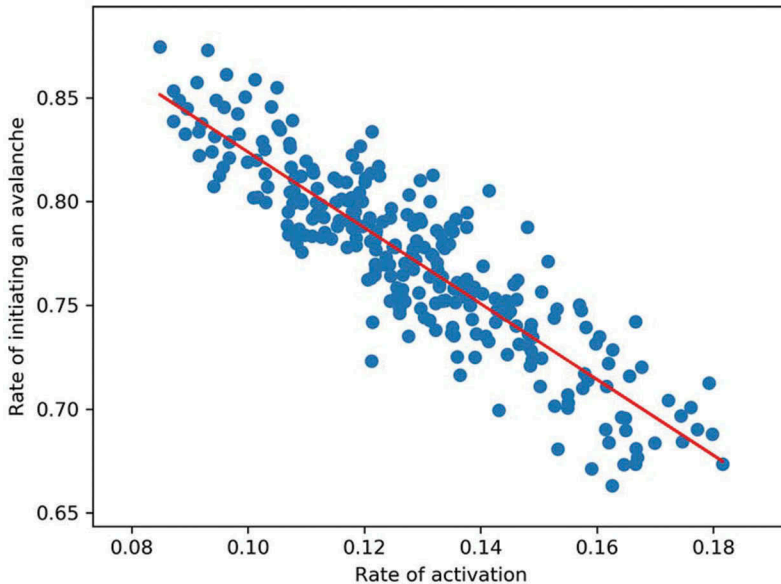


Figure 10. There is a negative correlation between rate of activation and rate of avalanche initiation ($r = -0.92, p < 0.001$).

trigger an avalanche. We also determined that these highly activated nodes are the high degree nodes, with a correlation coefficient of $r = 0.62$ ($p < 0.05$) between average degree and activation rate.

In a second series of analyses, we investigated the activation rates of individual neurons and average avalanche lengths initiated by each neuron. Avalanche length is the number of neurons activated during an avalanche. **Figure 11** shows the top 30 values. *C. elegans* is known to have a rich club comprising of 14 neurons (Towilson et al. 2013), whose names are *AVAL*, *AVAR*, *AVBL*, *AVBR*, *AVER*, *AVDR*, *AVEL*, *PVCL*, *PVCR*, *DVA*, *AVDL*, *AIBR*, *RIBL*, *RIAR*. Rich club of a network is a set of high-degree nodes with a preferential attachment to each other. Thus, the average path lengths among these nodes are shorter than the average. It may be observed that 10 out of 14 rich club neurons are among the top 30 highly activated neurons and the first 6 nodes are all rich club neurons. In terms of average avalanche length, 7 rich club neurons are among the top 30. This tells us that some neurons are more capable of generating long lasting avalanches whereas some others initiate shorter avalanches, and all in all they make the scale

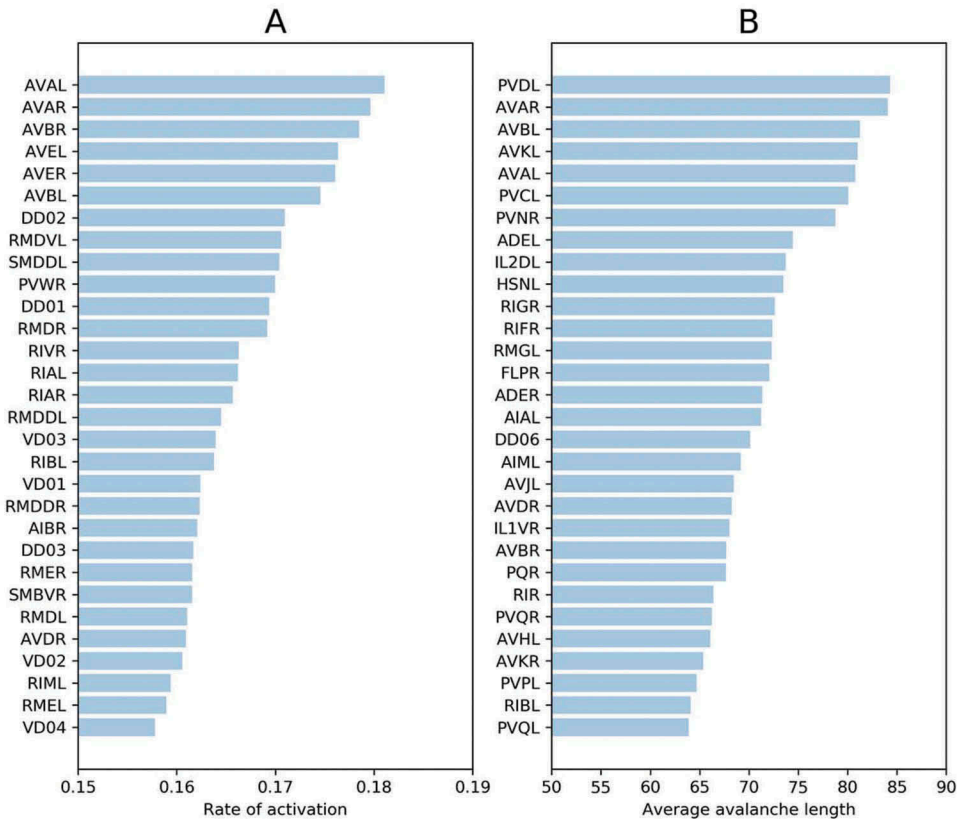


Figure 11. (A) Rate of activation. (B) average length of the avalanches initiated by a neuron. Vertical axes denote neuron names. (Top 30 values are shown.)

free avalanche distribution. However, further investigations should be made to reveal the relationships between the functional and structural properties of these neurons and their avalanche dynamics.

Discussion

Two assertions formed the basis of this study: first, noise controls the level of activity and hence is of functional importance for the nervous system (Buhman and Schulten 1987), and second, neuronal avalanches produced by SOC might be a new mode of network activity (Beggs and Plenz 2003). Motivated by these hypotheses, this study set out to explore the interactions between these two processes for the *C. elegans* neuronal network. The main finding is that an adaptive synaptic noise lends itself as a possible mechanism that drives the network towards SOC. Considering that there are various criticisms towards SOC theory (e.g., Frigg 2003). The results presented here do not supply any positive or negative evidence towards the existence SOC, but rather it claims that if SOC is indeed a mode of network activity, synaptic noise might be a mechanism that allows the anatomical network to generate dynamic functional topologies for SOC behaviour.

Experimental studies showed that synaptic failure probability is generally above 0.5 and can be well in excess of 0.9 (Allen and Stevens 1994; Hessler et al. 1993). The noise arising from the probabilistic nature of neurotransmitter release is actually an important mechanism of plasticity (Rosenmund and Clements 1993). The plasticity in terms of spike timing, its update rules, parameters have been explored both experimentally and analytically (Van Rossum et al. 2000). Consequently, we have a large set of feasible rules and parameters which allow the researchers to search for neurobiologically realistic determinants of SOC based on spike time-dependent plasticity (Rubinov et al. 2011). Synaptic noise was also shown to have a nonrandom component that modulates neuron function (Faure and Korn 1997). In this study, an update rule for this noise is proposed and tested on the neuronal network of *C. elegans*. The inclusion of the avalanche size as a synaptic failure update parameter constitutes the weakest point in all our modelling effort. The question of how a synapse gets information about the avalanche size is left unanswered in this study. A neuron gets information from other neurons that it has direct contact. Hence, a link between avalanche size and local activity profile should be sought. Providing global information to neural elements has also been a problem for neural models assigning spreading cascades along shortest paths. In a recent study, hubs and central pathways were shown to be dominating this shortest path activation (Mišić et al. 2015).

It should also be reiterated that the model used in this study is over simplistic. Nevertheless, it has been already been demonstrated that this type of simple models produced results in excellent agreement with more

realistic simulations (Messe et al. 2015). By abstracting away microscopic details, these types of simple models emphasize the emergence of global patterns from local neural interactions (Mišić et al. 2015). Moreover, similar models were efficiently employed to model the activity propagation in neural networks (Stam et al. 2015). The inclusion of the noise term actually drives our model closer to a variant of the forest fire model, in which immunity against fire is given to trees with some fixed probability (Clar et al. 1996).

Avalanches were hypothesized to be transient formation of cell assemblies (Plenz and Thiagarajan 2007). They represent spatially irregular patterns of propagated synchrony, which are stable and exhibit recurrence. The neuron chains shaped by the synaptic noise can be considered as a manifestation of these assemblies. As a post-hoc investigation, the distribution of failure probabilities were analysed to understand whether this distribution was similar across simulations. There were no significant correlations among the distributions. This observation indicates that neural networks might include many different overlapping functional assemblies capable of generating complex activation patterns.

Robust statistical assessment of power-law statistics is problematic with finite size systems (Taylor et al. 2013). In our model setting, since the driving of the neurons, i.e. transition from refractory to susceptible, stops during an avalanche, it is not possible for a neuron to reactivate within the same avalanche. This means that the maximum avalanche size (in terms of the number of activated neurons) is strictly limited by the network size. It is known that finite size systems exhibit a cut-off dictated by the system size (Plenz and Thiagarajan 2007). This was also evident in our results. However, for the critical regime a strong power-law behaviour was observed up to almost the network size.

Same model without the noise component and avalanche type activation revealed that activity in the neural network of *C. elegans* were dominated by central hub nodes (Muller-Linow et al. 2008). The well-defined activation sizes in our no-noise networks should be reconsidered in the future within this perspective. This behaviour might also be conceived as a manifestation of network-shaped self organization (Hutt et al. 2014). It was also observed that *C. elegans* neural network operated at a critical region rather than a certain critical point (Moretti and Muñoz 2013). In the present work, the existence of many different synaptic noise distributions each giving rise to critical behaviour might also be evaluated in the same light. Another point of concern is the structure-dynamics relationship of the *C. elegans* connectome. Our analyses showed that rich club of *C. elegans* neuronal network is active in creating the observed global avalanche dynamics, but further investigations are needed to explore these relationships. Relatedly, our analysis could not fully reveal which properties of the observed neural dynamics is inherent

to the neuronal network of *C. elegans* and which are not. Accordingly, proper analysis methods should be developed to better explore these points.

Note

1. For example, from www.openconnectomeproject.org, www.wormatlas.org.

References

- Achard S, Salvador R, Whitcher B, Suckling J, Bullmore E. 2006. A resilient, low-frequency, small-world human brain functional network with highly connected association cortical hubs. *J Neuroscience*. 26(1):63–72.
- Allen C, Stevens CF. 1994. An evaluation of causes for unreliability of synaptic transmission. *Proc Natl Acad Sci*. 91(22):10,380–10,383.
- Amaral LAN, Scala A, Barthelemy M, Stanley HE. 2000. Classes of small-world networks. *Proc Natl Acad Sci*. 97:11149–52.
- Bak P, Tang C, Wiesenfeld K. 1987. Self-organized criticality: an explanation of the 1/f noise. *Phys Rev Lett*. 59(4):381.
- Beggs JM, Plenz D. 2003. Neuronal avalanches in neocortical circuits. *J Neurosci*. 23(35):11,167–11,177.
- Buhmann J, Schulten K. 1987. Influence of noise on the function of a physiological neural network. *Biol Cybern*. 56(5–6):313–27.
- Clar S, Drossel B, Schwabl F. 1996. Forest fires and other examples of self-organized criticality. *J Phys: Condensed Matter*. 8(37):6803.
- Clauset A, Shalizi CR, Newman ME. 2009. Power-law distributions in empirical data. *SIAM Rev*. 51(4):661–703.
- Daniels BM, Krauker DC, Flack JC. 2017. Control of finite critical behaviour in a small-scale social system. *Nat Commun*. 8:14301.
- de Arcangelis L, Perrone-Capano C, Herrmann HJ. 2006. Self-organized criticality model for brain plasticity. *Phys Rev Lett*. 96(2):028107. doi:10.1103/PhysRevLett.96.028107.
- Drossel B, Schwabl F. 1992. Self-organized critical forest fire model. *Phys Rev Lett*. 69(11):1629.
- Droste F, Do AL, Gross T. 2012. Analytical investigation of self-organized criticality in neural networks. *J Royal Soc Interface*. 10(78):20120558.
- Faure P, Korn H. 1997. A nonrandom dynamic component in the synaptic noise of a central neuron. *Proc Natl Acad Sci*. 94(12):6506–11.
- Frigg R. 2003. Self-organised criticality: what it is and what it isn't. *Stud In Hist Philos Sci*. 34(3):613–32.
- Gatys LA, Ecker AS, Tchumatchenko T, Bethge M. 2015. Synaptic unreliability facilitates information transmission in balanced cortical populations. *Phys Rev E*. 91(6):062–707.
- Grassberger P. 2002. Critical behaviour of the Drossel-Schwabl forest fire model. *New J Phys*. 4(1):17.
- Hagberg AA, Schult DA, Swart PJ 2008. Exploring network structure, dynamics, and function using NetworkX. In: *Proceedings of the 7th Python in Science Conference (SciPy2008)*, Pasadena, CA USA, pp 11–15.
- Hesse J, Gross T. 2014. Self-organized criticality as a fundamental property of neural systems. *Front Syst Neurosci*. 8:166.
- Hessler NA, Shirke AM, Malinow R. 1993. The probability of transmitter release at a mammalian central synapse. *Nature*. 366(6455):569.

- Hunter JD. 2007. Matplotlib: A 2d graphics environment. *Comput In Sci Eng.* 9(3):90–95.
- Hutt MT, Kaiser M, Hilgetag CC. 2014. Perspective: network-guided pattern formation of neural dynamics. *Phil Trans R Soc B.* 369(1653):20130522.
- Jones E, Oliphant T, Peterson P, et al. (2001) SciPy: open source scientific tools for Python. [Online. accessed 2016 Feb 02]. URL <http://www.scipy.org/>
- Jung P, Hnggi P. 1991. Amplification of small signals via stochastic resonance. *Phys Rev A.* 44(12):8032.
- Laughlin SB, Sejnowski TJ. 2003. Communication in neuronal networks. *Science.* 301(5641):1870–74.
- Levina A 2008. A mathematical approach to self-organized criticality in neural networks. Nieders. Staatsu. Universitätsbibliothek Göttingen. Dissertation (Ph. D. thesis), webdoc.sub.gwdg.de/diss/2008/levina/levina.pdf.
- Lin M, Chen T. 2005. Self-organized criticality in a simple model of neurons based on small-world networks. *Phys Rev E.* 71(1):016133.
- Linkenkaer-Hansen K, Nikouline VV, Palva JM, Ilmoniemi RJ. 2001. Long-range temporal correlations and scaling behavior in human brain oscillations. *J Neuroscience.* 21(4):1370–77.
- Meisel C, Gross T. 2009. Adaptive self-organization in a realistic neural network model. *Phys Rev E.* 80(6):061917.
- Messe A, Hutt MT, Knig P, Hilgetag CC. 2015. A closer look at the apparent correlation of structural and functional connectivity in excitable neural networks. *Sci Rep.* 5:7870.
- Mišić B, Betzel RF, Nematzadeh A, Goni J, Griffa A, Hagmann P, Flammini A, Ahn YY, Sporns O. 2015. Cooperative and competitive spreading dynamics on the human connectome. *Neuron.* 86(6):1518–29.
- Moretti P, Muñoz MA. 2013. Griffiths phases and the stretching of criticality in brain networks. *Nat Commun.* 4:2521.
- Muller-Linow M, Hilgetag CC, Hutt MT. 2008. Organization of excitable dynamics in hierarchical biological networks. *PLoS Comput Biol.* 4(9):e1000190.
- Plenz D, Thiagarajan TC. 2007. The organizing principles of neuronal avalanches: cell assemblies in the cortex? *Trends Neurosci.* 30(3):101–10.
- Rosenmund C, Clements JD. 1993. Nonuniform probability of glutamate release at a hippocampal synapse. *Science.* 262(5134):754–57.
- Rubinov M, Sporns O, Thivierge JP, Breakspear M. 2011. Neurobiologically realistic determinants of self-organized criticality in networks of spiking neurons. *PLoS Comput Biol.* 7(6):e1002038.
- Stam C, van Straaten E, Van Dellen E, Tewarie P, Gong G, Hillebrand A, Meier J, Van Mieghem P. 2015. The relation between structural and functional connectivity patterns in complex brain networks. *Int J Psychophysiology.* 103:149–60.
- Taylor TJ, Hartley C, Simon PL, Kiss IZ, Berthouze L. 2013. Identification of criticality in neuronal avalanches: I. a theoretical investigation of the non-driven case. *J Math Neurosci.* 3(1):1–26.
- Teramae J, Fukai T. 2007. Local cortical circuit model inferred from power-law distributed neuronal avalanches. *J Comput Neurosci.* 22(3):301–12.
- Tononi G, Sporns O, Edelman GM. 1994. A measure for brain complexity: relating functional segregation and integration in the nervous system. *Proc Natl Acad Sci.* 91(11):5033–37.
- Towilson EK, Vértés PE, Ahnert SE, Schafer WR, Bullmore ET. 2013. The rich club of the *C. elegans* neuronal connectome. *J Neurosci.* 33(15):6380–87.
- Van Rossum MC, Bi GQ, Turrigiano GG. 2000. Stable Hebbian learning from spike timing-dependent plasticity. *J Neurosci.* 20(23):8812–21.
- Varshney LR, Chen BL, Paniagua E, Hall DH, Chklovskii DB. 2011. Structural properties of the *Caenorhabditis elegans* neuronal network. *PLoS Comput Biol.* 7(2):e1001066.

- Varshney LR, Sjostrom PJ, Chklovskii DB. 2006. Optimal information storage in noisy synapses under resource constraints. *Neuron*. 52(3):409–23.
- Wang SJ, Hilgetag CC, Zhou C. 2011. Sustained activity in hierarchical modular neural networks: self-organized criticality and oscillations. *Front Comput Neurosci*. 5:30.
- White JA, Rubinstein JT, Kay AR. 2000. Channel noise in neurons. *Trends Neurosci*. 23(3):131–37.